Preparation and Spectral, Electrochemical, and Photovoltaic Properties of Acene-Modified Zinc Porphyrins

Ching-Yao Lin,*,† Yu-Chien Wang,† Shun-Ju Hsu,‡ Chen-Fu Lo,† and Eric Wei-Guang Diau‡

Department of Applied Chemistry, National Chi Nan University, Puli, Nantou Hsien 545, Taiwan, and Department of Applied Chemistry and Institute for Molecular Science, National Chiao Tung University, Hsinchu 300, Taiwan

Received: September 25, 2009; Revised Manuscript Received: October 19, 2009

A series of acene-modified zinc porphyrins (benzene to pentacene, denoted as LAC-1 to LAC-5) were prepared to study their absorption spectra, electrochemical properties, and photovoltaic properties. For the absorption spectral changes in THF, porphyrin B bands are red-shifted and broadened from 449 to 501 nm for LAC-1 to LAC-3, showing the effect of additional π-conjugation. In contrast, the B bands of LAC-4 and LAC-5 are blue-shifted. In addition, the tetracenyl group of LAC-4 gives rise to absorption bands in between B and Q bands. On the other hand, the Q bands of LAC-1 to LAC-5 are systematically broadened and red-shifted from 629 to 751 nm. By comparison, the absorption bands of LAC porphyrins on TiO_2 films are broadened and slightly shifted. Fluorescence emission maxima of LAC porphyrins in THF are also systematically red-shifted from LAC-1 to LAC-5. Cyclic voltammetry experiments in THF/TBAP show that the first reductions are systematically positive-shifted from −1.16 to −0.85 V vs SCE for LAC-1 to LAC-5, indicating the effect of increasing π-conjugation. As for the performance of DSSCs using LAC porphyrins, the overall efficiencies are LAC-1 (2.95%), LAC-2 (3.31%), LAC-3 (5.44%), LAC-4 (2.82%), and LAC-5 (0.10%). Overall efficiency of a LAC-3-sensitized solar cell is nearly twice of that of a LAC-1-sensitized solar cell and is about 81% overall efficiency of N719-sensitized solar cells under the same experimental conditions. The conversion efficiency of incident photons to current (IPCE) experiments shows that the broadened absorption bands of LAC-3 effectively minimizes the gap between B and Q bands, contributing to the improved DSSC performance. The very poor performance of LAC-5 is suggested to be caused by rapid nonradiative relaxation of the molecule in the singlet excited state.

Introduction

Dye-sensitized solar cells (DSSC) have drawn much attention in recent decades.[1,2] Ru(II) complexes, such as the N3, N719, and C101 dyes, are the most efficient photosensitizers to date.[1b,3,4] Among the dyes under investigation, porphyrins are also considered for DSSC applications.[2b,c,5–9] The most efficient porphyrin-sensitized solar cell is reported by Officer and co-workers to have achieved an overall efficiency (η) of 7.1%.[5a] It has been suggested that applying dyes, such as porphyrins, with a high absorption coefficient can result in an efficient DSSC.[10] However, porphyrin absorptions are often narrow and with a gap between the B and Q absorption bands.[11] As a result, these properties limit the range of spectral response of porphyrin-sensitized solar cells and their performance in the gap region. We recently reported studies on a series of zinc porphyrins bearing linear, length-controlled phenyl-ethynyl anchoring groups (PE*x*, $x = 1-4$, see Chart 1 for the structure of PE1).[9] PE1 outperforms other porphyrins in the series ($\eta = 2.50\%$) and a gap at 500 nm too was observed in the UV−visible and photocurrent action spectra.[9a] Broadening the absorption bands may remedy this weakness of porphyrins, resulting in improved photovoltaic performance. There have been a few examples reported in the literature: Imahori and co-workers have shown that fusing naphthalene to a porphyrin led to a more efficient DSSC.[7] Zhou, Tamiaki, and co-workers recently also reported an efficient DSSC using oxo-bacteriochlorin for its broadband absorption capability.[12]

In this work, we systematically broaden porphyrin absorption bands with acenes and study the impacts to the UV−visible, electrochemical, and photovoltaic properties of the porphyrins. On the basis of our previous studies on PE*x* porphyrins, PE1 porphyrin was chosen to develop the next generation of photosensitizers. As shown in Chart 1, the new porphyrins (denoted as LAC-1−LAC-5) are essentially PE1 added one unit of acenyl-ethynyl group. For these porphyrins, zinc porphine acts as the primary chromophore. 3,5-Di-*tert*-butyl-phenyl groups are used to increase the solubility, to lessen aggregation, and to protect porphine core structure. Acenes (benzene to pentacene) are put between porphine and carboxylic anchoring group as the secondary chromophores in order to broaden porphyrin absorption bands. Scattered examples in the literature have shown that porphyrin absorption bands can be significantly affected by attaching phenyl-ethyne,[13,14] naphthylenyl-ethyne,[13] anthracenyl-ethyne,[14] and pentacenyl-ethyne[15] to the porphyrin meso positions. More importantly, the use of benzene to pentacene allows us to adjust absorption wavelengths of the secondary chromophore to observe the impacts of the acenes to porphyrin absorption spectra, i.e., a titration of porphyrin absorption bands by acenes.

Results and Discussion

Synthesis. Detailed synthetic procedure and compound characterization are described in the Supporting Information.

* To whom correspondence should be addressed. E-mail: cyl@ncnu.edu.tw.
† National Chi Nan University.
‡ National Chiao Tung University.

10.1021/jp909232b
Published on Web 11/09/2009

CHART 1: Structural Diagram of PE1 and LAC Porphyrins

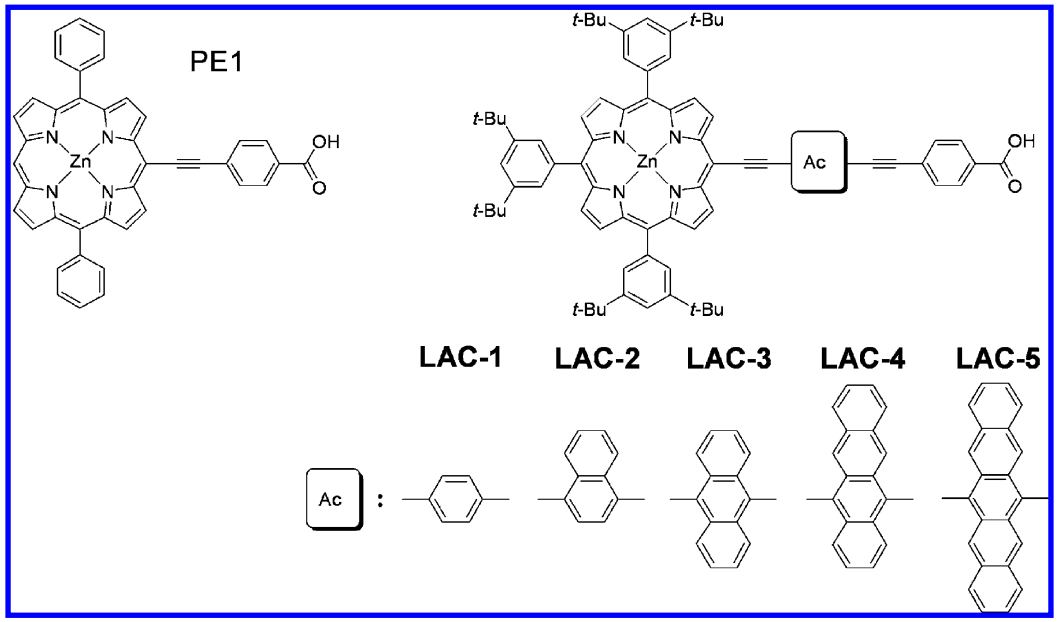

In brief, standard Sonogashira cross-coupling reaction or the copper-free method reported by Lindsey and co-workers were employed to prepare LAC-1−LAC-4.[16,17] The synthesis of LAC-1 is identical to that of PE2.[9a] For LAC-2−LAC-4, the synthesis was divided into two steps: In the first step, monobrominated porphyrin was cross-coupled to suitable acenyl-ethynyl precursors to yield the intermediate porphyrins. After purification, the intermediate porphyrins were reacted to 4-iodobenzoic acid to generate the final products. However, these methods did not work for LAC-5 due to the instability of pentacenyl-ethyne.[18] Therefore, one-pot reaction similar to the procedure described by Therien and co-workers[15] was employed to prepare LAC-5. Out of scientific curiosity, the one-pot reaction was also tested on LAC-4 and the yield was nearly twice of that of the two-step method.

UV−Visible and Fluorescence Spectral Properties. Figure 1a compares the UV−visible spectra of PE1 and acenyl-ethynyl precursors (denoted as <1> to <5>). Figure 1b overlays the UV−visible spectra of PE1 and LAC porphyrins. Figure 2 compares the absorption spectra of LAC porphyrins in THF with those on TiO_2 films in air. Figure 3 shows the fluorescence emission spectra of LAC porphyrins in THF. The wavelengths of UV−visible absorptions and fluorescence emissions are collected in Table 1.

For the acenyl-ethynyl precursors, the lowest-energy absorptions gradually red-shift from 293 to 639 nm as the conjugation system expands. This is consistent with the report by Anthony and co-workers.[19] Note that the wavelengths of <3> and <5> match those of PE1's B and Q bands, respectively, whereas the wavelengths of <4> locate between PE1's B and Q bands.

For LAC porphyrins, absorption bands are affected in each different fashion upon incorporating acenyl-ethynes into the π-conjugation system. These spectrum changes are consistent with the literature reports.[13–15] For LAC-1, the absorption bands are slightly red-shifted and intensified from those of PE1, indicating the effect of the additional phenyl-ethynyl conjugation. We also compare the UV−visible spectra of LAC-1 and PE2 because LAC-1 is essentially PE2 with two phenyl rings replaced by three 3,5-di-*tert*-butyl-phenyl groups. As shown in Table 1, the absorption bands of LAC-1 are also more red-shifted than those of PE2, showing the effect of three 3,5-di-*tert*-butyl-phenyl groups. For LAC-2, further red-shifts of the absorption bands and a splitting pattern of the B bands are observed. These spectrum changes are consistent with the expanded π-conjugation and the lowered molecular symmetry of the complex. For LAC-3, additional red-shifts of the absorption bands are observed for both B and Q bands. Remarkably, the split B bands spread out widely in the 400−500 nm region. For LAC-4, the B bands are not as red-shifted but the Q bands are red-shifted to 682 nm. In addition, the tetracene group gives rise to absorption bands at 513 and 554 nm, complementing the porphyrin B and Q bands. For LAC-5, the B bands are at 429 and 482 nm and the extremely broadened Q bands locate in the 500−800 nm region. The lowest-energy absorption band of LAC-5 might be an intramolecular charge transfer band because of the significant red-shift from the

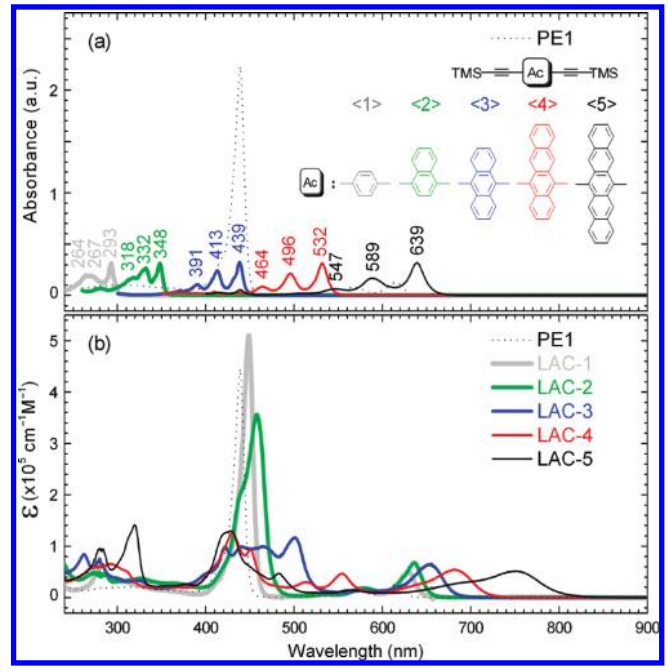

Figure 1. UV−visible spectra of (a) PE1 and the acenyl-ethynyl precursors, and (b) PE1 and LAC porphyrins in THF.

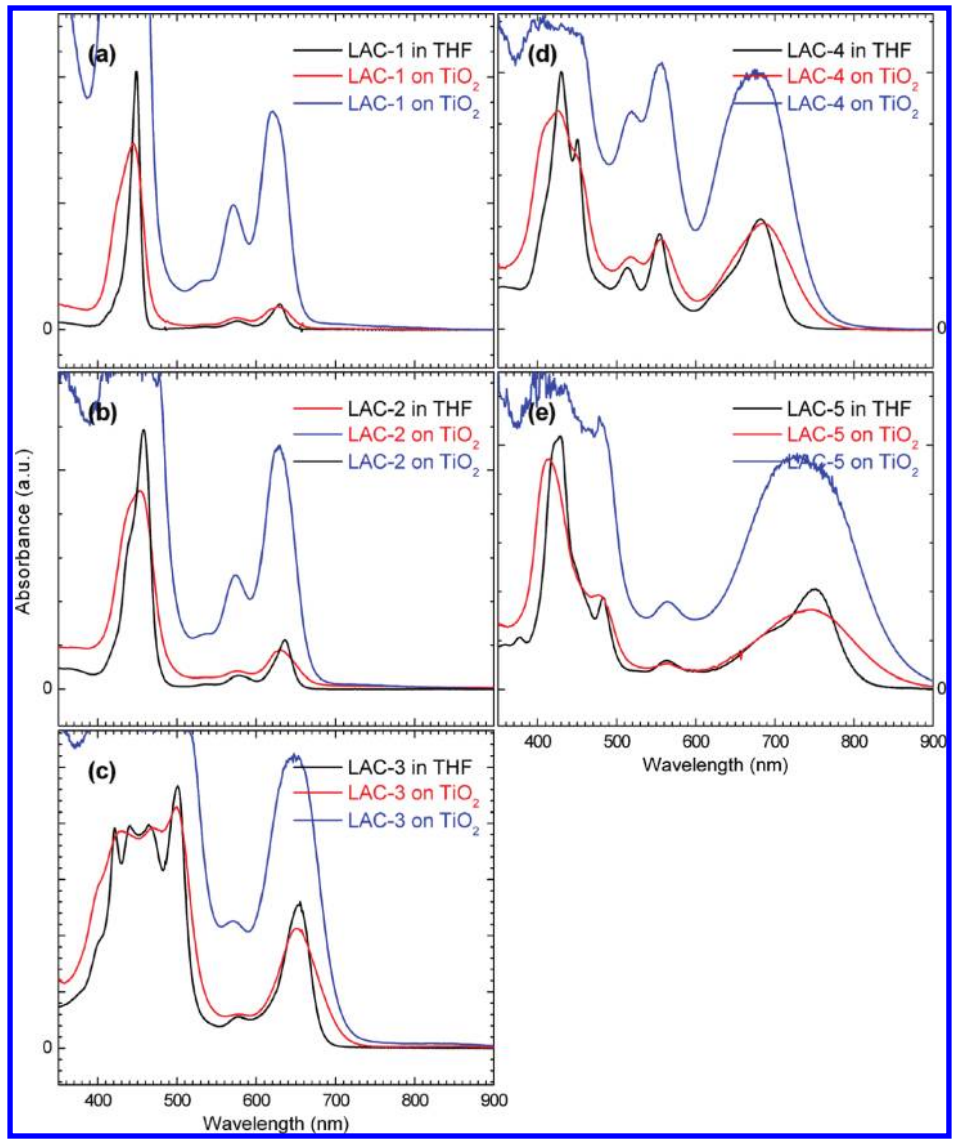

Figure 2. UV−visible spectra of (a) LAC-1, (b) LAC-2, (c) LAC-3, (d) LAC-4, and (e) LAC-5 porphyrins in THF (black curves) and on TiO_2 films in air (partially loaded, red curves; fully loaded, blue curves).

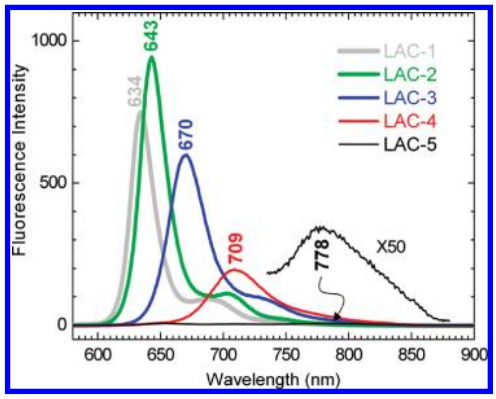

Figure 3. Fluorescence emission spectra of LAC-1 to LAC-5 in THF. Experimental conditions: [LAC-*x*] = 2×10^{-6} M; excitation wavelength (nm): LAC-1(449), LAC-2(458), LAC-3(501), LAC-4(430), and LAC-5(429).

component bands. It is noteworthy that LAC-3's B bands and LAC-5's Q bands are enormously broadened while the absorption wavelengths of <3> and <5> match those of PE1's B and Q bands, respectively. This implies that, for a fully conjugated system, matching the absorption wavelengths of the primary and secondary chromophores may result in significantly broadened absorption bands of the total system.

Figure 2 displays the UV−visible spectra of LAC porphyrins in THF (black curves) and on TiO_2 nanocrystalline films in air (partially loaded, red curves; fully loaded, blue curves). For the partially loaded spectra, only small amounts of the porphyrins were allowed to adsorb onto TiO_2 films in order to present both B and Q bands. In addition, these spectra were rescaled in order to qualitatively compare them in one figure. Comparison of the film with the solution spectra reveals that the Q bands of the LAC/TiO_2 films are only slightly shifted and considerably broadened from those of the solution spectra, whereas the B bands are also broadened with blue-shoulders. The broadened absorption bands of the film samples may be due to intermolecular interactions of the molecules aggregated on the TiO_2 surfaces. The blue-shoulders of the B bands are consistent with those of the PE*x* porphyrins. Therefore, they should be related to H-type aggregation of LAC porphyrins on the TiO_2 surfaces, i.e., LAC porphyrins "stand up" on the TiO_2 surfaces upon adsorption.[9] More importantly, the broadened absorption bands observed in the film spectra should help minimize the gap

TABLE 1: UV−Visible Absorption and Fluorescence[a] Maxima of PE1, PE2, and LAC Porphyrins in THF

dye	absorption, nm (log ε, 10^5 $M^{-1}cm^{-1}$)	emission, nm
PE1[b]	439(5.64), 567(4.21), 616(4.41)	621, 674
PE2[b]	443(5.67), 569(4.27), 619(4.60)	624, 678
LAC-1	449(5.72), 579(4.25), 629(4.72)	634, 688
LAC-2	458(5.48), 578(4.18), 636(4.76)	643, 703
LAC-3	421(4.99), 441(5.00), 464(5.00), 501(5.07), 580(4.15), 655(4.81)	670, 727
LAC-4	430(5.11), 450(4.98), 513(4.48)[c], 554(4.68)[c], 682(4.74)	709
LAC-5	429(5.12), 482(4.67), 564(4.14), 690(4.46), 751(4.72)	778

[a] Excitation wavelength (nm): LAC-1 (449), LAC-2 (458), LAC-3 (501), LAC-4 (430), and LAC-5 (429). [b] Taken from ref 9a. [c] Absorption bands from the tetracene group.

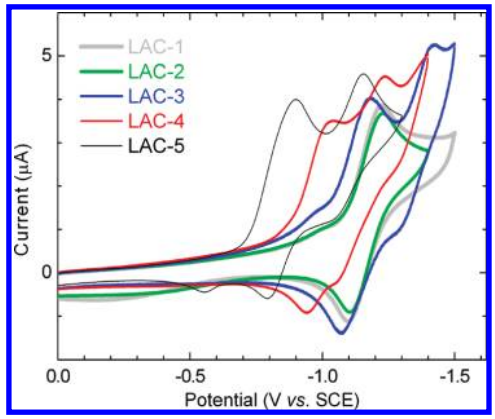

Figure 4. Cyclic voltammograms of 0.5 mM LAC porphyrins in THF/0.1 M TBAP.

TABLE 2: Reduction Potentials of PE1, PE2, LAC Porphyrins, and the Acenyl-ethyne Precursors[a]

	$E_{1/2}$, V vs SCE			$E_{1/2}$, V vs SCE	
dye	red(1)[b]	red(2)	precursor	red(1)	red(2)
PE1[c]	−1.23(130)				
PE2[c]	−1.18(125)				
LAC-1	−1.16(130)		<1>		
LAC-2	−1.15(130)		<2>		
LAC-3	−1.13(110)	−1.36(130)	<3>	−1.51(E_{pc})	
LAC-4	−0.99(100)	−1.15(180)	<4>	−1.13(200)	
LAC-5	−0.85(110)	−1.10(110)	<5>	−0.92(190)	−1.33(190)

[a] Experimental conditions: in THF/0.1 M TBAP under N_2.; Pt working and counter electrodes; SCE reference electrode; scan rate = 100 mV/s. Peak-to-peak separations (mV) are put in the parentheses for quasi-reversible reactions. For irreversible reductions, only the cathodic peak potentials (E_{pc}) are shown. [b] Porphyrin-ring reductions. [c] Taken from ref 9a.

between porphyrin B and Q bands, resulting in increased spectral responses of the solar cells (see below in the photovoltaic section).

Although the B bands of LAC porphyrins are differently affected by the acenyl-ethynyl bridges, the Q bands are systematically red-shifted from 629 to 751 nm as the π-conjugation increases. A similar trend is also observed in the fluorescence spectra: The fluorescence maxima red-shift from 634 to 778 nm for LAC-1 to LAC-5 (Figure 3 and Table 1). For LAC-4, the fluorescence emission is considerably weaker than those of LAC-1−LAC-3 and the shape of the emission band seems different from those of LAC-1−LAC-3. This may be related to the de-excitation processes of the molecule in the singlet excited state. It has been established that intersystem crossing (65%) and internal conversion (20%) are the major deactivation processes of tetracene in the singlet excited state, whereas fluorescence is the minor relaxation process (15%).[20] LAC-4 may also undergo these processes through electronic localization in the tetracenyl moiety (see below in the MO section), resulting in a weaker fluorescence emission. Similarly, the very weak fluorescence emission of LAC-5 can be related to the nonradiative de-excitation of the molecule in the singlet excited state. It has been established that internal conversion is the main deactivation mechanism of pentacene with a quantum yield greater than 75%.[20,21] LAC-5 may also undergo the nonradiative processes through electronic localization in the pentacenyl moiety, resulting in the very weak fluorescence emission.

Electrochemistry, Molecular Obital Patterns, and Energy Levels. Figure 4 overlays the cyclic voltammograms of LAC porphyrins in THF/TBAP. Reduction potentials of PE1, PE2, LAC porphyrins, and the acenyl-ethynyl precursors are collected in Table 2. Consistent with PE1 and PE2, the first porphyrin-ring reduction of LAC-1 in THF is a quasi-reversible reaction at −1.16 V vs SCE. As shown in the table, LAC-1 is easier to reduce than PE1, suggesting the effect of extending π-conjugation system. LAC-1 is also easier to reduce than PE2, showing the electron-donating influence of three 3,5-di-*tert*-butyl-phenyl groups over two phenyl rings. For LAC-2−LAC-5, the first porphyrin-ring reduction potentials are gradually positive-shifted from −1.15 to −0.85 V vs SCE, demonstrating the effect of expanding the size of acenes. Because of the anodic shifts of the reduction potentials, the second reductions were also observed for LAC-3, LAC-4 and LAC-5 at −1.36, −1.15, and −1.10 V, respectively. Oxidation reactions of LAC porphyrin in THF are irreversible reactions at room temperature.

In order to assist our qualitative understanding of the electrochemical behaviors of LAC porphyrins, we performed DFT calculations on LAC porphyrins at the B3LYP/LanL2DZ level.[22] Figure 5 depicts molecular orbital (MO) patterns of LAC-1−LAC-5 at HOMO-1−LUMO+1 levels. As shown in the figure, the MO patterns of LAC-1 are consistent with those of Gouterman's four-orbital model,[11] i.e., the HOMO-1 and HOMO resemble those of the a_{1u} and a_{2u} orbitals while the LUMO and LUMO+1 are similar to those of the e_g orbitals. Minor deviations are observed. For LAC-1, the HOMO and LUMO patterns are calculated to be mainly at the porphine core with slight delocalization to the anchoring group, suggesting the decreased symmetry of the complex and the extended π-conjugation of the substituent. For LAC-2, the MO patterns are similar to those of LAC-1 with very small MO patterns residing at the second ring of naphthalene. This is consistent with the small positive-shift of LAC-2 reduction potential. For LAC-3, the delocalization is calculated to be much more extensive at the HOMO and LUMO levels: As shown in the figure, the HOMO and LUMO patterns populate at both the porphine core and the anthracenyl-ethynyl anchoring group. The more delocalized LUMO pattern of LAC-3 is consistent with the further positive-shift of the reduction potentials. For LAC-4 to LAC-5, the MO patterns at the HOMO and LUMO levels become increasingly localized at the tetracenyl and pentacenyl

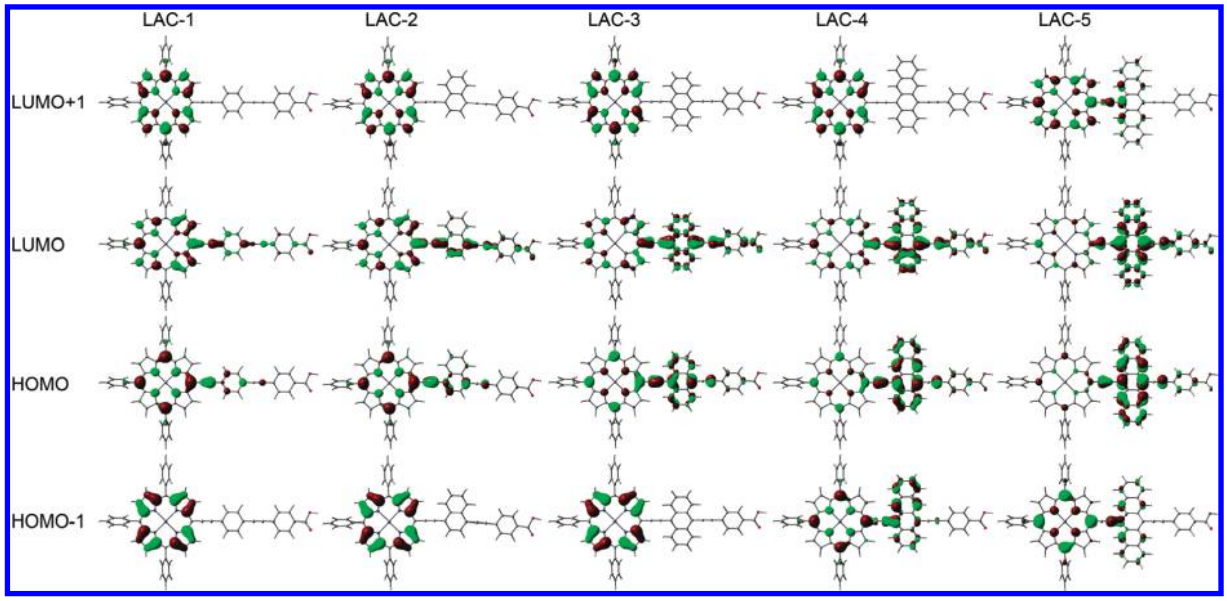

Figure 5. Molecular orbital patterns of LAC porphyrins with geometries of each molecule optimized at the B3LYP/LanL2DZ level of theory. Note that these MO patterns are used to qualitatively assist our understanding to the porphyrins.

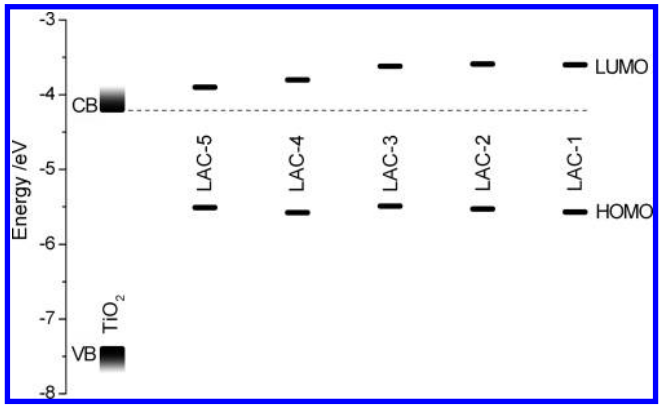

Figure 6. Energy-level diagram of LAC porphyrins and TiO_2.

groups, respectively. This is consistent with the CV and the fluorescence properties: As shown in Table 2, the first reduction potentials of LAC-4 and LAC-5 are determined to be −0.99 and −0.85 V, respectively. These potentials are closer to the reduction potentials of tetracene (−1.13 V) and pentacene (−0.92 V) precursors than that of PE1 (−1.23 V), suggesting that the first reduction reactions of LAC-4 and LAC-5 are more concentrated at the tetracenyl and pentacenyl groups, respectively. The increasing localization of π-orbitals may also affect the fluorescence emission of LAC-4 and LAC-5: As mentioned above, electronic localization in the tetracenyl and pentacenyl moiety may enable intersystem crossing and internal conversion to become the main channels of deactivation for LAC-4 and LAC-5 in the singlet excited state. Accordingly, fluorescence emission intensity of LAC-4 would be notably decreased and that of LAC-5 would be greatly diminished. This is consistent with the experimental results (Figure 3).

Figure 6 shows the energy-level diagram of LAC porphyrins and TiO_2, comparing the HOMO/LUMO of each porphyrin with the valence band (VB) and conducting band (CB) of TiO_2. This diagram is estimated according to the literature method:[2a] The first porphyrin-ring reduction potentials were used to estimate the LUMO levels. The UV−visible and the fluorescence spectra were used to estimate the gaps between the HOMOs and the LUMOs. This diagram shows that the LUMO levels of LAC porphyrins become more and more stabilized as the sizes of the acenes increase. Although the LUMO level of LAC-5 is the lowest in the series, it is still above the conducting bands of TiO_2. This suggests that the LUMO levels of LAC porphyrins should all be capable of injecting electrons to the conducting bands of TiO_2.

TABLE 3: Photovoltaic Parameters of LAC-Sensitized Solar Cells[a]

dye	J_{SC}/mA cm^{-2}	V_{OC}/V	*FF*	η (%)
LAC-1[b]	6.13 ± 0.04	0.67 ± 0.02	0.72 ± 0.01	2.95 ± 0.02
LAC-2	7.27 ± 0.41	0.65 ± 0.01	0.70 ± 0.02	3.31 ± 0.06
LAC-3	12.67 ± 0.46	0.67 ± 0.01	0.64 ± 0.03	5.44 ± 0.06
LAC-4	6.68 ± 0.05	0.61 ± 0.01	0.68 ± 0.01	2.82 ± 0.14
LAC-5	0.33 ± 0.06	0.49 ± 0.02	0.62 ± 0.05	0.10 ± 0.02
N719[c]	12.67 ± 0.91	0.74 ± 0.04	0.72 ± 0.02	6.73 ± 0.10

[a] Under AM1.5 illumination (power 100 mW cm^{-2}) with an active area of 0.16 cm^2. Three independent measurements were performed for all dyes using the TiO_2 films fabricated with an identical procedure in order to demonstrate the reproducibility of the data (see Supporting Information for the complete table). [b] Typical dye-loads of LAC-sensitized solar cells are estimated to be (in nmol/cm^2): 120 (LAC-1), 135 (LAC-2), 132 (LAC-3), 140 (LAC-4), and 140 (LAC-5). [c] As a reference, overall efficiency of N719 sensitized solar cell was also determined. The value is smaller than the literature value because of thinner TiO_2 films and without adding the scattering layer in our case.

Photovoltaic Properties. For the photovoltaic measurements, averaged photovoltaic parameters of LAC-sensitized solar cells are listed in Table 3. Figure 7 compares (a) photocurrent action spectra and (b) I−V curves of LAC-sensitized solar cells. In short, the overall efficiencies increase from LAC-1 (2.95%) to LAC-2 (3.31%) to LAC-3 (5.44%); however, overall efficiencies rapidly decrease to 2.82% of LAC-4 and 0.10% of LAC-5. Overall efficiency of LAC-3-sensitized solar cell is nearly twice of that of LAC-1-sensitized solar cell (2.95%) and is about 81% overall efficiency of N719-sensitized solar cells under the same experimental conditions. To further study the impacts of LAC absorption bands to the performance of the solar cells, we carried out the conversion efficiency of incident photons to current (IPCE) experiments. As shown in Figure 7a, the photocurrent action spectra are consistent with the UV−visible spectra. From LAC-1 to LAC-3, the responses in the B- and Q-band regions gradually broaden, intensify, and red-shift, contributing to the

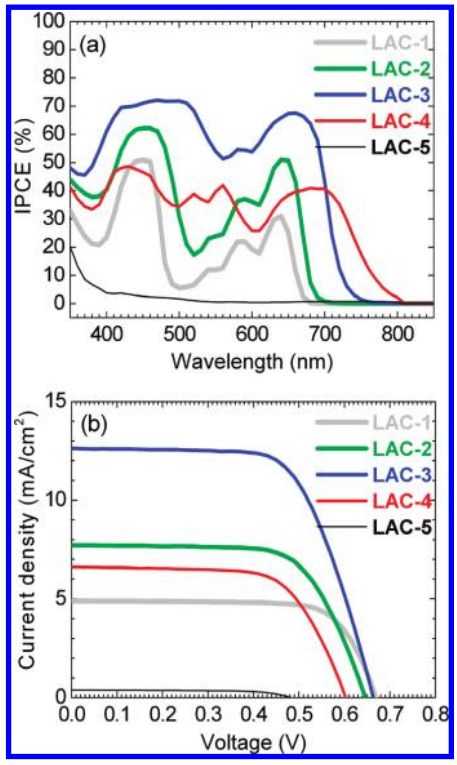

Figure 7. (a) Photocurrent action spectra and (b) I−V curves of LAC-sensitized solar cells. Corresponding overall efficiencies are 2.43% (LAC-1), 3.38% (LAC-2), 5.49% (LAC-3), 2.67% (LAC-4), and 0.12% (LAC-5) in these figures (not an averaged value).

higher photocurrents (J_{sc}, Figure 7b) and overall efficiencies. Note that the gap between B- and Q-band regions of LAC-3-sensitized solar cell is minimized owing to the broadened absorption bands. This is consistent with the broadened absorption bands of LAC-3/TiO_2 films (Figure 2c). For LAC-4, the presence of tetracene group complements porphyrin B and Q bands, and the combined absorption bands generate photocurrents beyond 800 nm. However, covering more wavelengths does not compensate the general drop of the IPCE and J_{sc} values. For LAC-5, the DSSCs also generate photocurrent beyond 800 nm. However, the IPCE values and J_{sc} are negligible in the visible region.

A few factors can be considered for the differences in the photovoltaic properties of LAC-sensitized solar cells: (1) As shown in Figure 5, the MO patterns of LAC-1 and LAC-2 at the HOMO and LUMO levels are more localized at the porphine core, whereas the MO patterns of LAC-3 are more evenly distributed at both the anthracenyl group and the porphine core. In contrast, the MO patterns of LAC-4 and LAC-5 at the HOMO and LUMO levels become increasingly localized at the acenyl groups. Compared with the photovoltaic results (LAC-1, η = 2.95%; LAC-2, η = 3.31%; LAC-3, η = 5.44%; LAC-4, η = 2.82%; and LAC-5, η = 0.10%), one would suggest that a delocalization of charge between the porphine core and the anthracene group at the HOMO level contributes to LAC-3's superior photovoltaic performance. (2) The improved photovoltaic performance of LAC-3-sensitized solar cell can also be found in the IPCE (Figure 7a) which is 50−70% in the 400−700 nm region. This would not be expected from the solution absorption spectrum because of a large gap between the B and Q bands (Figure 1b). This gap is not evident in the photocurrent action spectra possibly because of the considerably broadened film absorption bands (Figure 2c) or/and the scattering by TiO_2 nanoparticles which increases the photocurrents for the weak absorption in such a region. (3) The very poor performance of LAC-5-sensitized solar cell may be due to internal conversion of the pentacenyl group. It has been well established that internal conversion is the dominant deactivation process of pentacene with a quantum yield greater than 75%.[20,21] Because the frontier orbitals of LAC-5 are calculated to be largely localized at the pentacenyl group (Figure 5), LAC-5 might also undergo the nonradiative processes via electronic localization in the pentacenyl moiety, resulting in a very low electron injection yield and very poor photovoltaic performance.

Conclusion

We systematically demonstrate that porphyrin absorption spectra can be significantly affected by including acenes into the π-conjugation system. Among the acene-modified porphyrins, anthracene and pentacene groups substantially broaden porphyrin B (LAC-3) and Q (LAC-5) bands, respectively. On the other hand, tetracene group complements porphyrin absorption bands (LAC-4). For the performance of the DSSCs, the overall efficiencies first increase then decrease for LAC porphyrins: LAC-1 (2.95%) < LAC-2 (3.31%) < LAC-3 (5.44%) > LAC-4 (2.82%) ≫ LAC-5 (0.10%). LAC-3 outperforms other porphyrins in the series and overall efficiency of the DSSC is about 81% overall efficiency of N719-sensitized solar cells under the same experimental conditions. For LAC-3, IPCE and TiO_2 film spectrum show that broadening the absorption bands by anthracene effectively minimizes the gap between porphyrin B- and Q-band regions, contributing to the higher photocurrent and improved photovoltaic performance. Although LAC-5 also exhibits very broad absorption bands, the DSSC performs poorly. The very poor performance of DSSC using LAC-5 is suggested to be caused by nonradiative relaxation of the molecule in the singlet excited state. As a result, electron injection from LAC-5 to TiO_2 may not efficiently take place, rendering LAC-5 a poor photosensitizer.

Experimental Section

Materials. Air-sensitive solids were handled in an MBraun Unilab glovebox. A vacuum line and standard Schlenk techniques were employed to process air-sensitive solutions. Solvents used in the synthesis (ACS grade) were obtained from Mallinckrodt Baker, Inc. (CH_2Cl_2 and $CHCl_3$; Phillipsburg, NJ), Haltermann (hexanes; Hamburg, Germany), and Merck (THF; Darmstadt, Germany). These solvents were used as received unless otherwise stated. Other chemicals were ordered from Acros Organics (Morris Plains, NJ). THF was purified and dried by an Asiawong SD-500 Solvent Purification System (Taipei, Taiwan). Around 10 ppm of H_2O was found in the THF purified by the system. All NMR solvents were used as received. $Pd(PPh_3)_4$ catalyst was purchased from Strem Chemical Inc. (Newburyport, MA). $Pd_2(dba)_3$ was produced by Ultra Fine Chemical Technology Corp. Chromatographic purification was performed with Silica Gel 60 (230−400 mesh, Merck).

Instruments. NMR data were obtained on a Varian Unity Inova 300WB NMR spectrometer. Elemental analyses were carried out on an Elementar Vario EL III (NSC Instrumentation Center at National Chung Hsing University). Mass Spectroscopy measurements were performed on a Microflex MALDI-TOF MS (Bruker Daltonics). A CHI Electrochemical Workstation 611A was used to performed electrochemical measurements. Absorption spectra were recorded on an Agilent 8453 UV−visible spectrophotometry system. Fluorescence spectra were measured on a Varian Cary Eclipse fluorescence spectrophotometer.

Cell Fabrication and Performance Characterization. The porphyrin-based DSSC devices were fabricated with a TiO_2 nanoparticulated working electrode and a Pt-coated counter electrode. For a working electrode, a TiO_2 nanoparticulate film was produced on a fluoride-doped tin-oxide (FTO, 30 Ω/□, Sinonar, Taiwan) glass via screen printing. Crystallization of TiO_2 films (thickness ~12 μm and active area 0.16 cm^2) was performed on annealing in two stages: heating at 450 °C for 5 min followed by heating at 500 °C for 30 min. The electrode was then immersed in a porphyrin/THF solution (0.2 mM, 25 °C, 4 h) containing chenodeoxycholic acid (CDCA; 0.2 mm unless otherwise specified) for dye loading onto the TiO_2 film. The Pt counter electrodes were prepared by spin-coating drops of H_2PtCl_6 solution onto FTO glass and heating at 400 °C for 15 min. To prevent a short circuit, the two electrodes were assembled into a cell of sandwich type and sealed with a hot-melt film (SX1170, Solaronix, thickness 25 μm). The electrolyte solution containing LiI (0.1 M), I_2 (0.05 M), PMII (0.6 M), and 4-*tert*-butylpyridine (0.5 M) in a mixture of acetonitrile and valeronitrile (volume ratio 85:15) was introduced into the space between the two electrodes, therefore completing the fabrication of these DSSC devices. The performance of a DSSC device was assessed on measurement of an $I-V$ curve with an AM-1.5 solar simulator (Newport-Oriel 91160), which was calibrated with a Si-based reference cell (S1133, Hamamatsu) containing an IR-cut filter (KG5) to correct the spectral mismatch of the lamp. Three independent measurements were performed for all dyes using the TiO_2 films fabricated with an identical procedure in order to demonstrate the reproducibility of the data.

Acknowledgment. This work was supported by the National Science Council (NSC 97-2113-M-260-007-MY2 and NSC 97-2627-M-260-001). We also are grateful to the National Center for High-performance Computing for computer time and facilities.

Supporting Information Available: Synthesis and characterization of LAC porphyrins, CVs of the acenyl-ethynyl precursors, and detailed photovoltaic parameters of LAC-sensitized solar cells. This material is available free of charge via the Internet at http://pubs.acs.org.

References and Notes

(1) (a) O'Regan, B.; Grätzel, M. *Nature* **1991**, *353*, 737–740. (b) Wang, Q.; Ito, S.; Grätzel, M.; Fabregat-Santiago, F.; Mora-Seró, I.; Bisquert, J.; Bessho, T.; Imai, H. *J. Phys. Chem. B* **2006**, *110*, 25210–25221. (c) Grätzel, M. *Inorg. Chem.* **2005**, *44*, 6841–6851.

(2) For recent reviews: (a) Grätzel, M. *Nature* **2001**, *414*, 338–344. (b) Campbell, W. M.; Burrell, A. K.; Officer, D. L.; Jolley, K. W. *Coord. Chem. Rev.* **2004**, *248*, 1363–1379. (c) Imahori, H.; Umeyama, T.; Ito, S. *Acc. Chem. Res.*, 2009, Article ASAP.

(3) Nazeeruddin, M. K.; De Angelis, F.; Fantacci, S.; Selloni, A.; Viscardi, G.; Liska, P; Ito, S.; Takeru, B.; Grätzel, M. *J. Am. Chem. Soc.* **2005**, *127*, 16835–16847.

(4) Gao, F.; Wang, Y.; Shi, D.; Zhang, J.; Wang, M.; Jing, X.; Humphry-Baker, R.; Wang, P.; Zakeeruddin, S. M.; Grätzel, M. *J. Am. Chem. Soc.* **2008**, *130*, 10720–10728.

(5) Campbell, W. M.; Jolley, K. W.; Wagner, P.; Wagner, K.; Walsh, P. J.; Gordon, K. C.; Schmidt-Mende, L.; Nazeeruddin, M. K.; Wang, Q.; Grätzel, M.; Officer, D. L. *J. Phys. Chem. C.* **2007**, *111*, 11760–11762.

(6) Lee, C.-W.; Lu, H.-P.; Lan, C.-M.; Huang, Y.-L.; Liang, Y.-R.; Yen, W.-N.; Liu, Y.-C.; Lin, Y.-S.; Diau, E. W.-G.; Yeh, C.-Y. *Chem.—Eur. J.* **2009**, *15*, 1403–1412.

(7) (a) Eu, S.; Hayashi, S.; Umeyama, T.; Matano, Y.; Araki, Y.; Imahori, H *J. Phys. Chem. C,* **2008**, *112*, 4396–4405. (b) Hayashi, S.; M; Tanaka, Hayashi, H.; Eu, S.; Umeyama, T.; Matano, Y.; Araki, Y.; Imahori, H. *J. Phys. Chem. C,* **2008**, *112*, 15576–15585.

(8) (a) Rochford, J.; Chu, D.; Hagfeldt, A.; Galoppini, E. *J. Am. Chem. Soc.* **2007**, *129*, 4655–4665. (b) Park, J. K.; Lee, H. R.; Chen, J.; Shinokubo, H.; Osuka, A.; Kim, D. *J. Phys. Chem. C* **2008**, *112*, 16691–16699.

(9) (a) Lin, C.-Y.; Lo, C.-F.; Luo, L.; Lu, H.-P.; Hung, C.-S.; Diau, E. W.-G. *J. Phys. Chem. C* **2009**, *113*, 755–764. (b) Lo, C.-F.; Luo, L.; Diau, E. W.-G.; Chang, I.-J.; Lin, C.-Y. *Chem. Commun.* **2006**, 1430–1432.

(10) Robertson, N. *Angew. Chem., Int. Ed.* **2008**, *47*, 1012–1014, and references therein.

(11) Gouterman, M. *J. Mol. Spectrosc.* **1961**, *6*, 138.

(12) Wang, X.-F.; Kitao, O.; Zhou, H.; Tamiaki, H.; Sasaki, S.-I. *J. Phys. Chem. C* **2009**, *113*, 7954–7961.

(13) Kuo, M.-C.; Li, L.-A.; Yen, W.-N.; Lo, S.-S.; Lee, C.-W.; Yeh, C.-Y. *Dalton Trans.* **2007**, 1433–1439.

(14) Drobizhev, M.; Stepanenko, Y.; Dzenis, Y.; Karotki, A.; Rebane, A.; Taylor, P. N.; Anderson, H. L *J. Phys. Chem. B,* **2005**, *109*, 7223–7236.

(15) Susumu, K.; Duncan, T. V.; Therien, M. J. *J. Am. Chem. Soc.* **2005**, *127*, 5186–5195.

(16) (a) Sonogashira, K.; Tohda, Y.; Hagihara, N. *Tet. Lett.* **1975**, 4467–4470. (b) Takahashi, S.; Kuroyama, Y.; Sonogashira, K. *Synthesis* **1980**, 627–630.

(17) Wagner, R. W.; Johnson, T. E.; Li, F.; Lindsey, J. S. *J. Org. Chem.* **1995**, *60*, 5266–5273.

(18) Lehnherr, D.; McDonald, R.; Tykwinski, R. R. *Org Lett.* **2008**, *10*, 4163–4166, The asymmetrical functionalization method reported here unfortunately did not work for LAC-5.

(19) (a) Payne, M. M.; Parkin, S. R.; Anthony, J. E. *J. Am. Chem. Soc.* **2005**, *127*, 8028–8029.

(20) (a) Turro, N. J. *Modern Molecular Photochemistry*; University Science Books: Sausalito, CA, 1991; p 181. (c) Nijegorodov, N.; Ramachandran, V.; Winkoun, D. P. *Spectrochim. Acta, Part A* **1997**, *53*, 1813–1824. (d) Malkin, J. *Photophysical and Photochemical Properties of Aromatic Compounds*; CRC Press: Boca Raton, FL, 1992; pp 98—99.

(21) Orlowski, T. E.; Zewail, A. H. *J. Chem. Phys.* **1979**, *70*, 1390–1427.

(22) Frisch, M. J. *Gaussian 03, Revision D.01*; Gaussian, Inc.: Pittsburgh PA, 2003. All IR frequencies were checked to be positive.

JP909232B